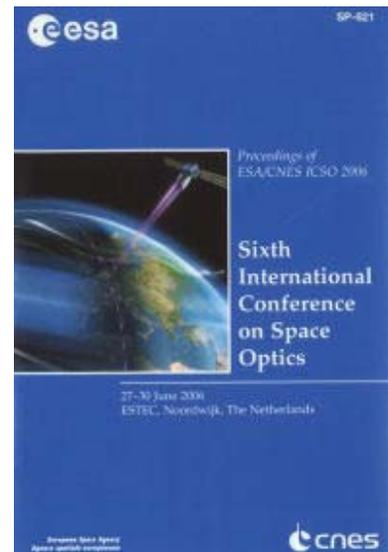# International Conference on Space Optics—ICSO 2006

Noordwijk, Netherlands

27–30 June 2006

Edited by Errico Armandillo, Josiane Costeraste, and Nikos Karafolas

Feasibility study on measuring axial and transverse stress/strain components in composite materials using Bragg sensors

G. Luyckx, J. Degrieck, W. De Waele, W. Van Paepegem, et al.

FEASIBILITY STUDY ON MEASURING AXIAL AND TRANSVERSE STRESS/STRAIN COMPONENTS IN COMPOSITE MATERIALS USING BRAGG SENSORS

G. Luyckx[(1)], J. Degrieck[(1)], W. De Waele[(1)], W. Van Paepegem[(1)]
[(1)]*Ghent University, Faculty of Engineering, Department of Mechanical Construction and Production Laboratory Soete, Sint-Pietersnieuwstraat 41, B-9000 Gent, Belgium, email: Geert.Luyckx@UGent.be*

J. Van Roosbroeck[(2)], K. Chah[(2)], J. Vlekken[(2)]
[(2)]*Fibre Optic Sensors and Sensing Systems (FOS&S), Cipalstraat 14, B-2440 Geel, Belgium, email: jvanroosbroeck@fos-s.com*

I. Mckenzie[(3)]
[(3)]*European Space Agency, Opto-electronics Section, ESTEC, TEC-MME, email: Iain.Mckenzie@esa.int*

A. Obst [(4)]
[(4)] *European Space Agency, ESTEC, TEC-MCS*
Postbus 299, 2200 AG Noordwijk, The Netherlands, email: Andreas.Obst@esa.int

Keywords: Structural health monitoring, Optical Fibre sensors, 3D-strain measurements

ABSTRACT

A fibre optic sensor design is proposed for simultaneously measuring the 3D stress (or strain) components and temperature inside thermo hardened composite materials. The sensor is based on two fibre Bragg gratings written in polarisation maintaining fibre. Based on calculations of the condition number, it will be shown that reasonable accuracies are to be expected. First tests on the bare sensors and on the sensors embedded in composite material, which confirm the expected behaviour, will be presented.

1. INTRODUCTION

During the last decades, there has been an increased use of fibre-reinforced composite materials for aerospace and space applications, thanks to their high stiffness for low weight and their excellent corrosion resistance. 'Damage tolerant' design of such structures necessitates permanent monitoring of the stresses or strains and the temperature in the composite material. Such monitoring systems should ensure the safety of the in-service aircraft, reduce 'time consuming' conventional non-destructive inspections and maximize the safety in case of life extension programs [1].
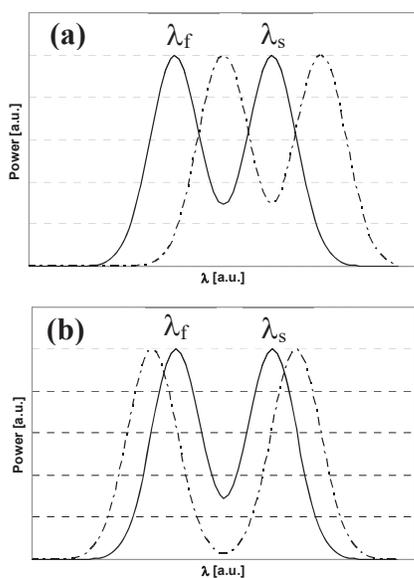
 It has been widely demonstrated in the international literature that optical fibres can be easily embedded into composite materials and that reliable and stable monitoring systems can be designed based on fibre Bragg grating (FBG) sensors [2]. The main advantages of the optical fibre technology are that the fibres are tiny (comparable to a human hair), explosion safe, immune against electromagnetic radiation, and

fairly corrosion resistant. In spite of some disadvantages of using embedded optical fibres (brittleness, composite material distortion, fragile connectorization), the authors believe that this technology is one of the most promising for online monitoring of the mechanical behaviour of composite structures. Most of the reported applications are based on single axial deformation measurements. It is, however, only feasible to monitor the occurrence and growth of damage when the entire 3D stress or strain state is known.

The following paragraphs report on the development of a sensor configuration based on FBG sensors, written in polarization maintaining fibres, for measuring multi-axial stresses (or strains) and temperature in thermo hardened composite elements. The expected accuracies are estimated, based on considerations of the condition number determined by the wavelength sensitivity values. Preliminary results of experiments on these multi-axial FBGs (bare as well as embedded in composite) will be presented and show the feasibility of the proposed sensor configuration.

2. MULTI AXIAL FBGS

In general, an FBG reflects a narrow part of the in-coupled broadband light spectrum. The wavelength of the reflected light shifts as a function of the applied axial strain or temperature and hence spectral analysis of the reflected light allows one to monitor axial strain or temperature changes. In case of FBG sensors written in birefringent fibres (polarisation maintaining fibre or PM fibre), both polarization modes will satisfy the Bragg condition at different wavelengths due to the difference in refractive index of the two polarization axes.

Therefore, FBGs written in such fibres will reflect two distinct peaks, one for each polarization axis. The peaks are normally indicated with the names 'fast' and 'slow', corresponding to the propagation speed of light along both polarisation axes of the PM fibre. The separation of the two peaks is directly proportional to the birefringence of the fibre. A change in axial strain or temperature will not affect the birefringence of the fibre but will cause an overall shift of the refractive indices towards higher or lower values. It results in a similar shift in Bragg wavelength for the peaks from both polarization axes, as shown in Fig. 1a. If on the other hand a change in transversal strain is applied, a change of the birefringence of the fibre will occur and this results in a change of the peak separation, shown in Fig. 1b [3]. Depending on the direction of the applied transversal strain with respect to the polarisation axes of the fibre, the peak shift will increase or decrease.

Fig. 1. Effect on the spectral response of a PM-FBG due to (a) axial stress or uniform temperature change and (b) transverse stress.

In general, the fibre will be exposed to both longitudinal and transverse strains and to temperature changes. The corresponding shifts of the fast and slow Bragg wavelengths are given by Eq. 1 [4].

$$\begin{cases} \dfrac{\Delta\lambda_f}{\lambda_f} = GF1_{\varepsilon,x}\Delta\varepsilon_x + GF2_{\varepsilon,x}\Delta\varepsilon_y + GF3_{\varepsilon,x}\Delta\varepsilon_z + \alpha_x\Delta T \\[2mm] \dfrac{\Delta\lambda_s}{\lambda_s} = GF1_{\varepsilon,y}\Delta\varepsilon_x + GF2_{\varepsilon,y}\Delta\varepsilon_y + GF3_{\varepsilon,y}\Delta\varepsilon_z + \alpha_y\Delta T \end{cases}$$

Eq. 1

The GF-coefficients are the so-called gauge factors and they are characteristic for the FBG-sensor [4].

They can be determined using a calibration procedure, in which transversal and axial stresses (or strains) are varied. Similarly, the temperature sensitivity coefficients α can be determined in a temperature calibration procedure. This type of sensor enables the measurement of two Bragg-wavelengths and hence yielding the potential of determining two strain-components. In order to determine the 3D-strain components ε_x, ε_y and ε_z, at least 2 sensors of this type are required. The two sensors yield 4 measurable wavelengths what allows the determination of a fourth parameter (e.g. the temperature) as well.

3. PROPOSED SENSOR CONFIGURATION

By using a second grating written in the same fibre, one gets a set of equations like in Eq. 2.

$$\begin{bmatrix} \Delta\lambda_{s,1} \\ \Delta\lambda_{f,1} \\ \Delta\lambda_{s,2} \\ \Delta\lambda_{s,2} \end{bmatrix} = K \begin{bmatrix} \Delta\varepsilon_x \\ \Delta\varepsilon_y \\ \Delta\varepsilon_z \\ \Delta T \end{bmatrix}$$

Eq. 2

The K-matrix is the result of the unstrained wavelengths multiplied by the matrix of gauge factors and temperature coefficients. It is given by Eq. 3.

$$K = \begin{bmatrix} \lambda_{s,1} & 0 & 0 & 0 \\ 0 & \lambda_{f,1} & 0 & 0 \\ 0 & 0 & \lambda_{s,2} & 0 \\ 0 & 0 & 0 & \lambda_{f,2} \end{bmatrix} \begin{bmatrix} GF1_{\varepsilon,x,1} & GF2_{\varepsilon,x,1} & GF3_{\varepsilon,x,1} & \alpha_{x,1} \\ GF1_{\varepsilon,y,1} & GF2_{\varepsilon,y,1} & GF3_{\varepsilon,y,1} & \alpha_{y,1} \\ GF1_{\varepsilon,x,2} & GF2_{\varepsilon,x,2} & GF3_{\varepsilon,x,2} & \alpha_{x,2} \\ GF1_{\varepsilon,y,2} & GF2_{\varepsilon,y,2} & GF3_{\varepsilon,y,2} & \alpha_{y,2} \end{bmatrix}$$

Eq. 3

The linear set of equations from Eq. 2 can - in principle - be solved in order to derive the 3D strain components and the temperature. Pure mathematically spoken, a unique solution of the set of equations exists on the condition that the matrix K is non-singular i.e. if its determinant differs from zero. In practice, it is the degree of non-singularity, expressed by the condition number of the matrix, which determines the accuracy of the calculated solution.

The condition number of a square non-singular matrix A with respect to a given norm is defined as in Eq. 4. Here, ‖A‖ represents the norm of the matrix A.

$$Cond(A) = \|A\| * \|A^{-1}\|$$

Eq. 4

The norm can be computed e.g. as the maximum absolute column sum, like in Eq. 5.

$$\|A\| = max_i \sum_{j=1}^{n} |a_{ij}|$$

Eq. 5

The condition number of a matrix is always positive and greater than or equal to 1. For the identity matrix, the condition number equals one; for a singular matrix, the condition number equals infinity.

When the sensor is made out of two identical FBGs written in the same fibre, the gauge factors for both sensors will be linearly dependent which will result in a large condition number. In the here proposed sensor configuration, one of the two FBGs will be placed inside a capillary, as illustrated in Fig. 2. The capillary is meant to shield the FBG from transverse strains. In this way, both FBGs will react differently on external strains, what improves the condition number of the matrix greatly.
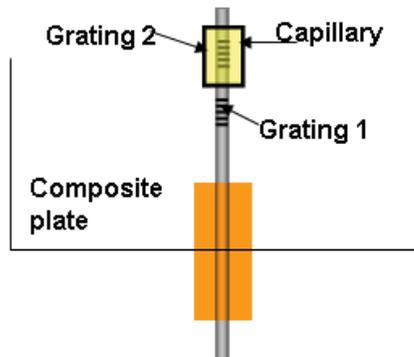

Fig. 2. The proposed sensor configuration.

In the ideal case, the capillary should isolate the FBG from transversal stresses. If the FBG is not entirely shielded from transverse stress, one expects the condition number to deteriorate [5].

To illustrate this, the condition numbers were calculated for the proposed sensor configuration for various degrees of isolation to transverse stress. For the K-matrix, the values were derived from [6], where the different sensitivities of a Bow-Tie fibre sample were derived. The condition numbers are presented in Table 1 and they indeed increase for decreasing degrees of isolation.

The table also presents the expected accuracies, provided that the measuring unit has a 1 pm accuracy for determining the Bragg wavelengths. It should be noted that the temperature sensitivities from the K-matrix derived from [6] only showed a small difference (α_x=15.0 pm/°C and α_y=15.7 pm/°C). Nevertheless, the derived accuracies are pretty satisfactory. They are optimal for a 100% degree of isolation. Hence, maximum isolation by the capillary is preferred.

Table 1: Calculated condition number and corresponding accuracies for various degrees of isolation to transverse stress.

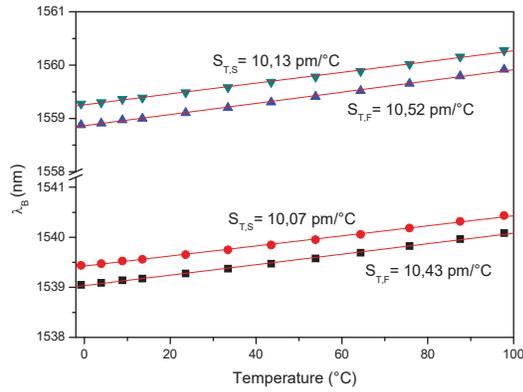| Isolation to Transverse Stress [%]	Condition Number	Accuracy		
		Transverse Strain [µε]	Axial strain [µε]	Temp. [°C]
25	133	18.9	111	7.8
50	112	9.4	49.5	3.5
75	108	6.3	30.4	2.2
100	105	4.7	22	1.6

4. SENSOR CALIBRATIONS

First tests were done to validate the feasibility of the proposed sensor design. FBGs were written in two types of PM-fibre: Panda and Bow-Tie. Their properties are summarized in Table 2.

Table 2: Properties of the PM-fibres and capillaries used for the first tests.

		Panda	Bow-Tie
Fibre	Cladding [µm]	125	80
	Coating [µm]	245	165
	Coating type	acrylate	acrylate
	Birefringence [10^{-4}]	3.2	3.9
Capillary	Inner diameter [µm]	320	184
	Outer diamater [µm]	560	334
	Polyimide coating [µm]	16	18

Different samples were prepared, each containing one or several pairs of FBGs. Prior to writing, the fibre samples were hydrogenated during 5 days at 70°C and 200 bar. Before inscription, the acrylate coating was locally removed. Inscription was done with a Talbot interferometer with the use of a KrF Excimer laser emitting at 248 nm. After the writing process, the FBGs were annealed at 100°C for 12 hours in order to stabilise the grating reflectivity. After the annealing, some FBGs were acrylate recoated; others were left uncoated. For each FBG-pair, one FBG was placed in a polyimide coated fused silica capillary (see Table 2). Glue was placed at both ends of the capillary in order to prevent the liquid composite material (epoxy) to enter the capillary during the embedding process.
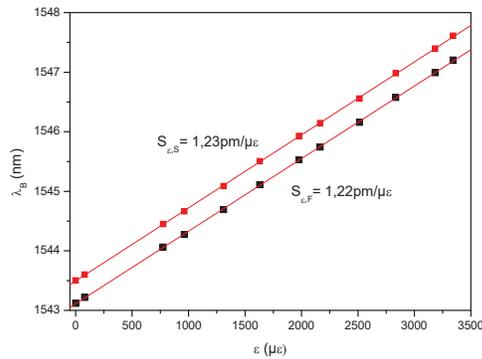
The bare sensors obtained in this way were then calibrated for their response to temperature and axial and transverse stress. A typical graph obtained for the temperature calibration for two FBGs is presented in Fig. 3.

Fig. 3. Temperature dependence of the fast and slow axes for two FBGs in a Bow-Tie fibre.

It can be seen that the slow and fast axes show slightly different sensitivities for each FBG. This was observed for all examined samples. The difference is in the range of 0.4 pm/°C and is comparable to the difference observed in [6].
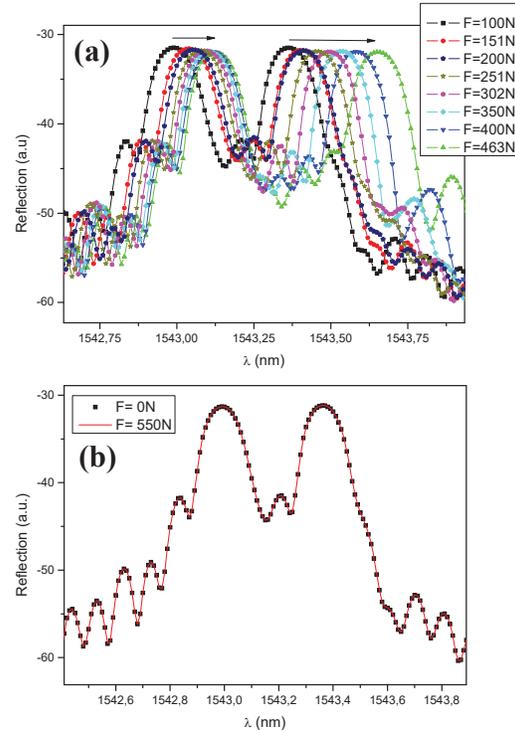
The axial strain calibration was performed using a strain bench where the fibre was submitted to different loads. Knowing the Young modulus and the cross-section of the fibre then allowed to calculate the applied strain. An example of an axial strain calibration is shown in Fig. 4. It can be seen that the sensitivities for both axes are nearly identical.

Fig. 4. Axial strain dependence of the fast and slow axes for one FBG in a Bow-Tie fibre.

For the transverse strain calibration, the fibre was mounted on two rotational stages and transverse loads were then applied to the fibre. Depending on the rotation angle of the stages, the position of both polarization axes with respect to the applied load could be varied. It was observed that the capillary gave excellent protection against transverse loads, as illustrated in Fig. 5. The figure shows the measured spectra for different transverse loads applied along the slow axis of a Panda fibre. In part (a), the FBG is without capillary and one observes the different shifts of the fast and slow peaks as expected. Preliminary transverse stress calibrations

were done but they showed to be of poor quality. Improved calibrations will be done by making modifications on the calibration bench. In part (b), the FBG is inside a capillary and one observes no shift whatsoever between the loaded (550 N) and unloaded conditions. The good isolation characteristics of the capillary were also predicted by finite element modelling, see [7].

Fig. 5. Reflection spectra of a Panda fibre for different applied transverse loads for (a) a bare FBG and (b) an FBG inside a capillary.

5. EMBEDDED SENSORS

First tests with the multi-axial sensors embedded in a composite material were performed and showed similar results as for the bare sensors. A picture of a composite sample containing the capillary-based sensor is shown in Fig. 6. The temperature calibration curves for the fast and the slow wavelengths of both FBGs are presented in Fig. 7. The FBGs were written in a Bow-Tie fibre.

One notices that the temperature sensitivities are slightly reduced compared to those derived for the bare sensor (Fig. 3). These differences could be explained by the thermal expansion of the composite material. Thermal expansion effects are expected to be the smallest for the FBG inside the capillary because of the isolation from the transverse stresses. Hence, the deviation of the temperature sensitivity is also smallest for this FBG. Notice however that there is again a small difference in sensitivity of roughly 0.4 pm/°C between the fast and slow axes. This is necessary for a good conditioning of the K-matrix.

In order to determine the response to axial stresses, the composite sample was clamped from both sides in a calibration setup, where different pulling forces could be applied. The results are presented in Fig. 8.

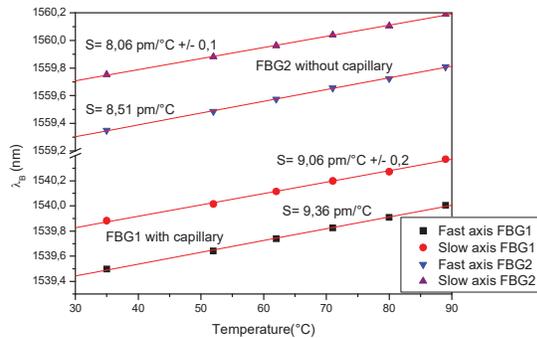**Fig. 6. Picture of a composite sample containing the capillary based sensor design of Fig. 2.**

Fig. 7. Temperature calibration curves for the fast and slow wavelengths of both FBGs from the embedded sensor.

The sensitivities for both axes and for both FBGs are comparable. This is as expected since the capillary should only affect transversal and not axial forces.
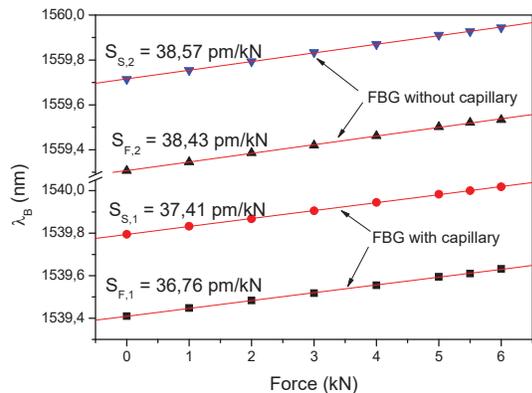

Fig. 8. Axial stress calibration for the FBGs inside the composite sample.

Transverse stress calibrations were done by applying known forces in the direction of the composite surface. The measured transverse stress calibrations are presented in Fig. 9. The peaks from the FBG without capillary show a clear dependence on the applied load whereas the peaks from the FBG inside the capillary show only a weak load dependence, hence the capillary is shielding the FBG from transversal stresses. The fact that there is a small dependence can be explained because the applied transversal strain of the composite induces a small elongation in the perpendicular direction due to the Poisson effect.
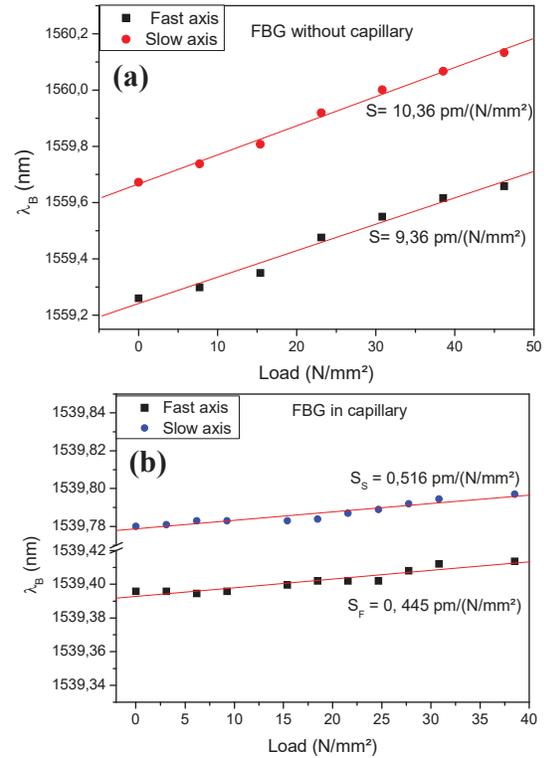

Fig. 9. Transverse stress calibration curves for the FBG without (a) and with (b) capillary.

CONCLUSION

A sensor design was proposed for measuring 3D strain/stress and temperature inside composite materials. The sensor is based on two identical FBGs written in PM-fibre, which lead to 4 measurable wavelengths which can be related to the strain and temperature via a matrix equation. The importance of a good conditioning of the matrix was stressed: to achieve reasonable accuracies, it is imperative that both FBGs show different sensitivities to the strain/stress components and temperature. A different sensitivity to transversal stresses could be achieved by putting one FBG inside a capillary. It was shown that the capillary indeed is capable of doing so, also when it is being embedded inside composite material. Next to a difference in transversal strain sensitivity, it was

also shown that the temperature sensitivity for both polarization axes was slightly different. A small but important difference of roughly 0.4 pm/°C could be observed between the fast and the slow axis, both for the bare as for the embedded sensors. It proves that the proposed sensor is indeed capable of measuring the 3D strain/stress components and the temperature. In the future, more elaborate measurements will be performed in order to fully characterize the responses of the embedded sensors.

ACKNOWLEDGEMENTS

REFERENCES

1. Schmidt H.-J., Telgkamp J., Schmidt-Brandecker B., "Application of structural health monitoring to improve efficiency of aircraft structure", The 2nd European workshop on Structural Health Monitoring, Munich, July 7-9 2004

2. De Waele W., Degrieck J, Baets R, Moerman W, and Taerwe L., "Load and deformation monitoring of composite pressure vessels by means of optical fibre sensors", *Insight* 43 (8) 518-525, 2001.

3. Luyckx, G.; De Waele, W.; Degrieck, J., "Multi-axial stress and strain sensing with Bragg-sensors: a theoretical study" proc. ACOMEN 2005, Ghent, 2005.

4. Luyckx, G.; De Waele, W.; Degrieck, J., Vlekken J., Chah K., "Multi-axial Fibre Bragg sensors for monitoring purposes", unpublished conference proceeding ECCM12, Biaritz.

5. J. Vlekken, J. Vermeiren, W. De Waele, "Multi-Axial Stress and Strain Sensing with Fibre Optic Sensors", Critical Design Report, ESA-contract 19026/05/NL/I.

6. Chehura E *et al.*, "Characterization of the response of fibre Bragg gratings fabricated in stress and geometrically induced high birefringence fibres to temperature and transverse load", *Smart Materials and Structures* 13 (2004) 888-894

7. Luyckx G.; De Waele W.; Van Paepegem W.; Degrieck J.; Vlekken J.; Chah K, "Feasibility study on discriminating axial and transverse stress/strain components with Bragg sensors", to be published in the conference proceedings of the 3rd European Workshop on Structural Health Monitoring, Granada, Spain, 2006.